Seismo-electromagnetic phenomenon in the atmosphere in terms of 3D subionospheric radio wave propagation problem

O.V. Soloviev [a,*], M. Hayakawa [b], V.I. Ivanov [a], O.A. Molchanov [c]

[a] *Institute of Radiophysics, St. Petersburg State University, Ul'yanovskaya 1/1, Petrodvorets, St. Petersburg 198504, Russia*
[b] *Department of Electronic Engineering, The University of Electro-Communications, 1-5-1 Chofugaoka, Chofu Tokyo 182-8585, Japan*
[c] *United Institute of Physics of the Earth RAS, Bol. Gruzinskaya 10, Moscow 123810, Russia*

Abstract

This paper presents a mathematical model, an asymptotic theory and an appropriate numerical algorithm to study, in the scalar approximation, VLF point source field propagation problem within the non-uniform Earth-ionosphere waveguide. We have taken into account a 3D local ionospheric inhomogeneity over the ground of the solar terminator transition. The local ionospheric perturbation whose centre is situated above the model earthquake, is simulated by a bell-shaped impedance inhomogeneity of the ionospheric waveguide wall. The ionosphere model parameters are computed with allowing for the geomagnetic field. Our numerical results show that the inclusion of the local ionospheric inhomogeneity in the radio wave propagation across the solar terminator path deforms the diurnal variations of field amplitude and phase in accordance with the observational data.
© 2004 Elsevier Ltd. All rights reserved.

1. Introduction

The possibility of existence of ionospheric precursory signatures of earthquakes is more and more accepted. Various ionospheric plasma phenomena have been detected by satellites and ground-based facilities over the epicentre of future shocks (Hayakawa and Molchanov, 2002). The applications of subionospheric VLF radio signals in a search for the seismic hazard precursors are widely discussed in the literature. In the context of VLF radio wave propagation the most important ionospheric parameters are the height profiles of electron density and effective collision frequency. These parameters in the regular conditions are determined by solar zenith angle. The spatially localized variations of electron density (due to various causes) are possible in the perturbed conditions, but so far we still do not understand clearly the nature of seismic influence on the ionosphere.

Monitoring of the "OMEGA" signals at the Inubo observatory (35°42′N; 140°52′E) from the Tsushima transmitter (34°37′N; 129°27′E) at both 10.2 and 11.3 kHz frequencies revealed a time shift of the regular minima in the diurnal variations of phase and amplitude for the propagation path 1043 km long, which can be considered as short-distance propagation (Hayakawa et al., 1996a,b; Molchanov and Hayakawa, 1998; Molchanov et al., 1998). The minima in the diurnal phase and amplitude patterns generally occur when the terminator moves along the VLF propagation path (the day–night boundary is nearly perpendicular to the transmitter–receiver direction). One minimum takes place around sunrise and can be named morning "terminator time" (TT); another takes place around sunset and can be named as evening TT. Those TT values might change from day to day as the day length at a given geographic latitude, if the propagation path is latitudinal. In the case of earthquake influence, there occurred the abnormal behaviour of this morning and evening TT difference, which began a few days before the earthquake such that it had lengthening of daytime conditions (Hayakawa et al., 1996a,b; Molchanov and Hayakawa, 1998; Molchanov et al., 1998).

The solar terminator is a part of terrestrial atmosphere situated between the space illuminated by the full ball of the sun and the complete shadow space. It is a layer between two conical surfaces, and the layer boundaries are very diffuse. The strongest variations

* Corresponding author.
E-mail address: soloviev@ovs.usr.pr.ru (O.V. Soloviev).

of temperature, pressure, and electron density height profile in the atmosphere during all natural days occur at the passage of solar terminator (Somsikov and Ganguly, 1995). It conveys the suggestion that the ionospheric plasma is unstable during the period of terminator transition, and hopefully it is possible to receive an appreciable response to an extraneous action (originated from seismic activity) into this region and this response may be powerful enough to be recorded. And the central idea of the TT method lies in high sensitivity of VLF signals to those changes in the lower ionosphere due to multimode interaction when the evening or morning terminator moves along a propagation path.

Let us return to the curves of VLF field amplitude and phase diurnal variations. These well-known curves for a given transmitter, recorded at the observation point away from the transmitter by some distances, have exhibited defined deformations during the time preceding a seismic event (Hayakawa et al., 1996a,b). It has been the case when the propagation path is not too long (about 1000 km) and has passed through the domain of seismic event, or the epicentre zone has been within the first Fresnel zone. We may consider this experimental result as significant (Hayakawa, 2001), however, up to now there is no complete theoretical understanding of the recorded phenomenon. In the literature there are some papers that present arguments supporting the existence of coupling between the recorded VLF field anomaly due to ionospheric perturbation, and earthquake precursor (Nikolaenko et al., 1999; Molchanov et al., 2001), while there are some papers that suspect this coupling (Clilverd et al., 1999; Rodger and Clilverd, 1999). Rodger and Clilverd (1999) consider in greater detail the modelling previously applied (Hayakawa et al., 1996a,b; Molchanov et al., 1998) and investigate the application of more sophisticated numerical propagation code to the same homogeneous waveguide model. In all the calculation presented in their papers the assumption has been made that the earthquake induced TT change is affected by the entire propagation path. This model must be admitted rather crude for the propagation path when the terminator drives along. The calculation in the modelling by Clilverd et al. (1999) is performed for a rather long (12 Mm) propagation path. We have an opinion that the perturbed area by earthquake precursor in the ionosphere is very small as compared with the scale of this path length, and that is why it is impossible to expect its appreciable influence on the signal phase and/or amplitude. So the conclusions of Clilverd et al. (1999) based on the long wave propagation capability code (LWPC) (Ferguson and Snyder, 1990) are rather questionable.

The attempts of theoretical explanation of observed result on the deformation of amplitude and phase diurnal curves made to date are based on the two-dimensional solutions of the propagation problem in an irregular Earth-ionosphere waveguide. In this paper we present a solution of the three-dimensional subionospheric radio wave propagation problem. We intend to show that the deformations of VLF field amplitude and phase diurnal variations may be explained by emergence of the local lower ionosphere inhomogeneity above the epicentre of the seismic event. This is a goal of our paper. As in the experiment described in Hayakawa et al. (1996a,b) we will have an interest in short enough paths (approximately 1000 km) oriented in the west-east direction. The scales of three-dimensional local lower ionosphere inhomogeneity (longitudinal, transverse and vertical) are chosen to be less than the terminator transition length.

2. Formulation of the propagation problem

Modelling the effects of the terminator is a special problem in the theory of subionospheric VLF propagation that has been often discussed in the literature (Wait, 1968a,b; Galejs, 1971; Pappert and Morfitt, 1975; Smith, 1977; Novikov and Rybachek, 1997). Most frequently the problem of VLF propagation in an irregular (in the direction of propagation) Earth-ionosphere waveguide (including day-time to night-time transitions) was considered with the aid of the modified transverse sections method, wherein the irregular waveguide is approximated by a set of regular parts (Galuk and Ivanov, 1978). This method is based on normal mode theory. The distances between the source (or receiver) and the nearest waveguide discontinuity must be much greater than a wavelength. The number of regular parts and their length depend on the required accuracy of the field component calculations (in practice the length of the regular part at the signal frequency of about 10 kHz is taken as a few hundred kilometres). The sophisticated codes on the basis of this method are most suitable for calculating long-range propagation at VLF, but they do not provide correct results for short distances from the source and so it does not apply to our case. Therefore we will make use of surface integral equation method, which was not applied for such a kind of propagation problems as we know. The same method allows us to take into account the effect of a local upper ionosphere inhomogeneity (possibly applied to earthquake precursor) on the electromagnetic field in the terrestrial waveguide.

The problem of subionospheric radio wave propagation in the presence of a localized irregularity has already been discussed for a long time. In Soloviev and Hayakawa (2002) we have given a detailed list of publications devoted to modelling the effect of three-dimensional ionospheric irregularities on the near-Earth propagation of radio waves.

This paper puts forward a three-dimensional modelling of radio wave propagation in an irregular wave-

guide with a localized inhomogeneity on the terminator background. The scales of three-dimensional local lower ionosphere inhomogeneity (longitudinal, transverse and vertical) are chosen to be less than the terminator transition length. The geometry of the problem is illustrated in Fig. 1. The Earth's surface is considered as uniform all through the propagation path and is characterized by a homogeneous surface impedance δ_g. The ionospheric surface impedance δ_{it} and waveguide height z_{it} for terminator transition model are obtained from the given electron density $N_e(z, \Psi)$ and effective collision frequency $v_e(z, \Psi)$ height profiles (Orlov et al., 2000; Earth's Lower Ionosphere, 1995), which depend on the solar zenith angle Ψ that varies from 80° to 100° with a step equal to 2°. It means that we explore the terminator transition with about 2500 km. The examples of such height profiles predicted for January, 1995 and for the central point of Tsushima–Inubo propagation path are given in Fig. 2, with the electron density height profiles in the upper panel and the effective electron collision frequency in the lower panel. The two curves in the upper panel correspond to different solar zenith angle; one is for $\Psi = 80°$ (daytime electron density) and the other for $\Psi = 100°$ (night-time electron density). Only one effective collision frequency height profile is used for all $80° \leqslant \Psi \leqslant 100°$ (Fig. 2, lower panel).

In the cylindrical coordinate system (r, φ, z) the functions $z_{it} = z_{it}(r, \varphi)$ and $\delta_{it} = \delta_{it}(r, \varphi, z_{it})$ do not change in the direction perpendicular to the terminator movement direction. These functions z_{it} and δ_{it} defining the ionosphere transition model are computed allowing for the geomagnetic field influence. Upon the ground of the solar terminator a three-dimensional local ionosphere inhomogeneity S_p is assumed above the propagation line. This last one is a bell-shaped perturbation of the ionospheric waveguide wall, whose centre is situated above the given point of the Earth's surface and whose lateral dimensions are less than the solar terminator transition length. The local ionosphere inhomogeneity S_p deforms the surface $S_{it}(z_{it} = z_{it}(r, \varphi))$ into the surface S_i described by the function $z_i = z_i(r, \varphi)$ and with

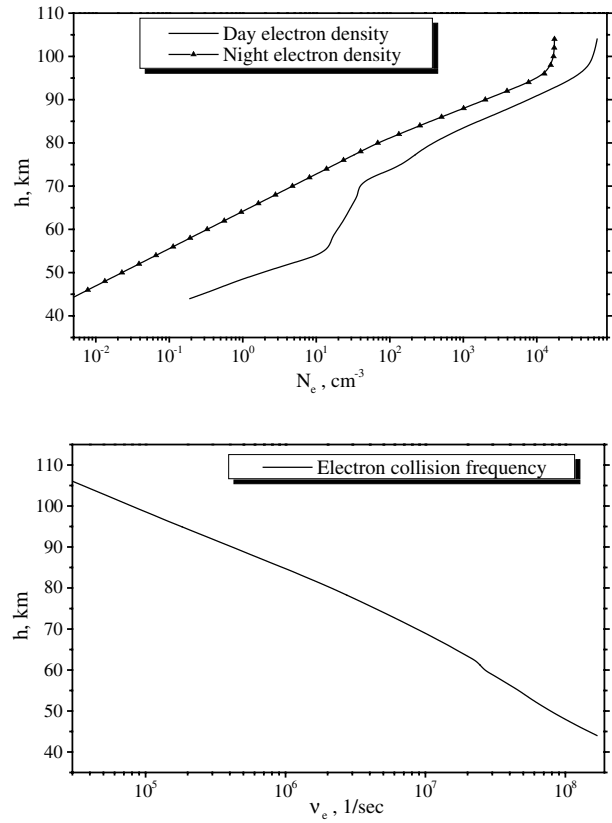

Fig. 1. Geometry of the problem.

Fig. 2. The examples of electron density (upper panel) and effective collision frequency (lower panel) height profiles that are used to calculate the effective terrestrial waveguide model parameters.

impedance $\delta_i = \delta_i(r, \varphi, z_i)$. Thus, the surfaces S_{it} and S_i coincide with each other everywhere with exception of the area $S_p \in S_i$ which defines the surface of the local inhomogeneity.

We study a harmonic $\exp(-i\omega t)$ point source field in the three-dimensional domain D bounded by two surfaces S_g and S_i. The source is assumed to be an electric dipole with moment P_0 located at the point described as $(x = 0, y = 0, z = z_t)$ in the Cartesian coordinate system and as $(r = 0, \varphi = 0, z = z_t)$ in the cylindrical coordinate system. The dipole is chosen to be directed along the axis OZ. The surface S_g is specified as $z = 0$, and so we neglect the Earth's curvature in our model (because our propagation path is not too long). As well, we simplify the problem and do not take into account the vector effects. We may therefore characterize the electromagnetic field by the scalar function $\Pi(x, y, z)$, the vertical component of Hertz's vector, which satisfies the Helmholtz equation in D and the following impedance boundary condition:

$$\frac{1}{\Pi} \frac{\partial \Pi}{\partial n} = \mathrm{i}k\delta(M)\Big|_{M \in S_g, S_i, S_p}, \tag{1}$$

where $k = \omega\sqrt{\varepsilon_0\mu_0}$ is the free-space wave number, n is the outside normal to the waveguide volume D, and
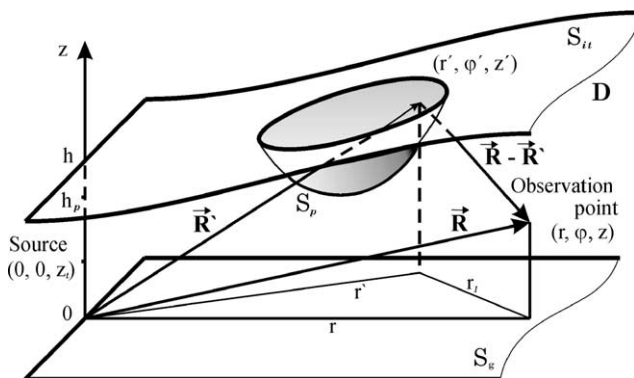
$\delta(M)$ is an inhomogeneous surface impedance function $(Re\,\delta > 0)$: $\delta(M) = \delta_g$ if $M \in S_g$, $\delta(M) = \delta_i(r, \varphi, z_i)$ if $M \in S_i$, and $\delta(M) = \delta_p(r, \varphi, z)$ if $M \in S_p$. The infinity condition requires $\Pi(r, \varphi, z)$ to vanish as $r \to \infty$. The vertical electric field component E_z can be obtained from the following equation:

$$E_z(r, \varphi, z) = (k^2 + \partial^2/\partial z^2)\Pi(r, \varphi, z).$$

The function E_z satisfies the same Helmholtz equation in D and the boundary conditions similar to Eq. (1) (Fok, 1965). However, $\Pi(r, \varphi, z)$ as a function of r has the weaker singularity at the zero point than E_z, that simplifies the solution construction for $\Pi(r, \varphi, z)$. Soloviev (1999, 2000) has discussed a quite different vector statement of the problem that requires to handle directly the electromagnetic field components.

3. Theory and computational algorithm

Using the second Green's formula, the unknown function $\Pi(r, \varphi, z)$ may be related to the solution of the regular problem $\Pi_0(r, z)$ by a surface integral over the surface S_i:

$$\Pi(\vec{R}) = \Pi_0(\vec{R}) + \frac{ik\varepsilon_0}{P_0} \int\int_{S_i} \Pi(\vec{R}')\left[\delta_i(\vec{R}')\Pi_0(\vec{R}, \vec{R}')\right.$$
$$\left. + i\frac{\partial \Pi_0(\vec{R}, \vec{R}')}{k\partial n'}\right] dS', \qquad (2)$$

where $\vec{R}(r, \varphi, z) \notin S_i$ is the observation point, $\vec{R}'(r', \varphi', z') \in S_i$ is an integration point, n' is a normal directed outside the waveguide cavity D, and $\Pi_0(\vec{R})$ is the field in the regular waveguide characterized by the height h ($h \geqslant z_i$) and by homogeneous impedance values $\delta_g = \text{const}$ and $\delta_{i0} = \text{const}$. $\Pi_0(\vec{R}, \vec{R}')$ is the Green's function obtained from $\Pi_0(\vec{R}, \vec{R}') = \Pi_0(\vec{R}_1)$ where $\vec{R}_1 = \vec{R} - \vec{R}'$ and $r_1 = \sqrt{r^2 + r'^2 - 2rr'\cos(\varphi - \varphi')}$ (see Fig. 1).

Together with the main problem and Eq. (2) we may write the equation for the propagation problem without any local perturbation S_p and taking into account only the terminator transition and we obtain Eq. (3):

$$\Pi_t(\vec{R}) = \Pi_0(\vec{R}) + \frac{ik\varepsilon_0}{P_0} \int\int_{S_{it}} \Pi_t(\vec{R}')\left[\delta_{it}(\vec{R}')\Pi_0(\vec{R}, \vec{R}')\right.$$
$$\left. + i\frac{\partial \Pi_0(\vec{R}, \vec{R}')}{k\partial n'}\right] dS'. \qquad (3)$$

The algorithm of the solution of Eq. (2) may be the following. First of all we transform the surface integrals from right-hand side of the last Eqs. (2) and (3) which are the surface integrals of the first type (Fihtenholtz, 1969), into the ordinary two-dimensional integrals over $z = \text{const}$ plane.

$$\int\int_{S_i} f(x', y', z')\,dS'$$
$$= \int\int_{\Omega_i} f(x', y', z_i'(x', y'))\sqrt{1 + p_p^2 + q_p^2}\,dx'\,dy'.$$

Here Ω_i is the (x, y) plane projection of the surface S_i; $p_p = \frac{\partial z_i'(x', y')}{\partial x'}$, $q_p = \frac{\partial z_i'(x', y')}{\partial y'}$. We separate the plane Ω_i into two parts: Ω_p and Ω_∞ ($\Omega_i = \Omega_p \cup \Omega_\infty$), where the first Ω_p is the (x, y) plane projection of the local perturbation surface S_p and for the second, which is the all-remaining part of the plane Ω_i, we have the coincidence of the functions z_i and z_{it} and δ_i and δ_{it}, i.e. for $x, y \in \Omega_\infty$ we have $z_i(x, y) = z_{it}(x, y)$, and $\delta_i(x, y, z) = \delta_{it}(x, y, z)$ (see Fig. 3).

Subtracting Eq. (2) with transformed surface integral from Eq. (3) similarly transformed we finally arrive at the equation:

$$\Pi(\vec{R}) = \Pi_0(\vec{R}) + \frac{ik\varepsilon_0}{P_0} \int\int_{\Omega_p + \Omega_\infty} \Pi(\vec{R}')\left(\delta_{it}(\vec{R}')\Pi_0(\vec{R}, \vec{R}')\right.$$
$$\left. + i\frac{\partial \Pi_0(\vec{R}, \vec{R}')}{k\partial n'}\right)\sqrt{1 + p_t^2 + q_t^2}\,dx'\,dy' + \frac{ik\varepsilon_0}{P_0}$$
$$\times \int\int_{\Omega_p} \Pi(\vec{R}')\left[\left(\delta_{it}(\vec{R}')\Pi_0(\vec{R}, \vec{R}') + i\frac{\partial \Pi_0(\vec{R}, \vec{R}')}{k\partial n'}\right)\right.$$
$$\times \sqrt{1 + p_p^2 + q_p^2} - \left(\delta_{it}(\vec{R}')\Pi_0(\vec{R}, \vec{R}')\right.$$
$$\left.\left. + i\frac{\partial \Pi_0(\vec{R}, \vec{R}')}{k\partial n'}\right)\sqrt{1 + p_t^2 + q_t^2}\right] dx'\,dy', \qquad (4)$$

where $p_{t,p} = \frac{\partial z_{it,i}'(x', y')}{\partial x'}$, $q_{t,p} = \frac{\partial z_{it,i}'(x', y')}{\partial y'}$, $\vec{R} \notin S_i$. In a limiting case $\vec{R} \to S_i$ an additional item $\Pi(\vec{R})/2$ arises on the right-hand side of Eq. (4) due to a jump in the normal derivative of the Green's function $\partial \Pi_0(\vec{R}', \vec{R})/\partial n'$.

To solve (4), we apply the asymptotic method (Soloviev, 1998). We begin with introducing the slowly varying attenuation functions V and V_0:

$$\Pi(\vec{R}) = \frac{P_0}{2\pi\varepsilon_0}\frac{e^{ikr}}{r}V(\vec{R}),$$
$$\Pi_0(\vec{R}, \vec{R}') = \frac{P_0}{2\pi\varepsilon_0}\frac{e^{ikr_1}}{r_1}V_0(\vec{R}, \vec{R}'). \qquad (5)$$

Then we introduce on the surface (x, y) an elliptic coordinate system (u, v) with focuses at the points: the origin $(0, 0)$ and observation point plane projection $(r, 0)$
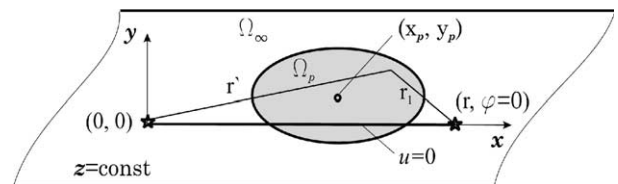

Fig. 3. Geometry of the problem, top view.

$$x' - \frac{r}{2} = \frac{r}{2}\mathrm{ch}u\cos v, \quad y' = \frac{r}{2}\mathrm{sh}u\sin v,$$

$$\mathrm{d}x'\,\mathrm{d}y' = r'r_1\,\mathrm{d}u\,\mathrm{d}v, \quad -\infty < u < +\infty, \quad 0 \leqslant v \leqslant \pi.$$

After substitution of the variables of integration we arrive at Eq. (6) for the slowly varying attenuation function V:

$$V(\vec{R}) = V_0(\vec{R}) + \frac{\mathrm{i}kr}{2\pi}\int\int_{\Omega_i} f_t(\vec{R},u,v)\mathrm{e}^{\mathrm{i}kr(\mathrm{ch}u-1)}\,\mathrm{d}u\,\mathrm{d}v$$

$$+ \frac{\mathrm{i}kr}{2\pi}\int\int_{\Omega_p} f(\vec{R},u,v)\mathrm{e}^{\mathrm{i}kr(\mathrm{ch}u-1)}\,\mathrm{d}u\,\mathrm{d}v. \tag{6}$$

If we suppose $kr \gg 1$, the exponential factor $\mathrm{e}^{\mathrm{i}kr(\mathrm{ch}u-1)}$ may be assumed as being rapidly oscillating with respect to u (across the wave propagation path) as compared with the remaining cofactor $f_t(\vec{R},u,v)$ and $f(\vec{R},u,v)$. This allows us to use the method of stationary phase for calculating the integrals over u. Before we apply the method of stationary phase, we need to transform the integrals from (6). The Eqs. (7)–(9) present the sequential steps of this operation:

$$\int\int_{\Omega_i} \cdots \mathrm{d}u\,\mathrm{d}v = \int_0^\pi \left(\int_{-\infty}^{+\infty} \cdots \mathrm{d}u\right)\mathrm{d}v, \tag{7}$$

$$\int\int_{\Omega_p} \cdots \mathrm{d}u\,\mathrm{d}v = \int_{v_<}^{v_>} \left(\int_{u_<(v)}^{u_>(u)} \cdots \mathrm{d}u\right)\mathrm{d}v, \tag{8}$$

$$\int_{u_<(v)}^{u_>(v)} \cdots \mathrm{d}u = \int_{u_<(v)}^\infty \cdots \mathrm{d}u - \int_{u_>(v)}^\infty \cdots \mathrm{d}u. \tag{9}$$

The line $u = 0$, which connects the plane projections of the source and the observation points, is a stationary phase point for infinite and semi-infinite integrals. To avoid losing the information on the transverse structure of the inhomogeneity, we must perform the stationary phase calculations with accuracy up to the terms of order $\mathrm{O}((kr)^{-1})$, neglecting only higher-order terms $\mathrm{O}((kr)^{-3/2})$. Thus, we have

$$\int_{-\infty}^{+\infty} f_t(\vec{R},u,v)\mathrm{e}^{\mathrm{i}kr(\mathrm{ch}u-1)}\,\mathrm{d}u \approx f_t(\vec{R},0,v)\mathrm{i}\pi H_0^{(1)}(kr), \tag{10}$$

$$\int_{u(v)}^\infty f(\vec{R},u,v)\mathrm{e}^{\mathrm{i}kr(\mathrm{ch}u-1)}\,\mathrm{d}u$$

$$\approx \frac{\exp[\mathrm{i}kr(\mathrm{ch}u(v)-1)]}{\mathrm{i}\sqrt{2kr}} \times G(\vec{R},u(v),v) + \mathrm{O}[(kr)^{-3/2}], \tag{11}$$

where $H_0^{(1)}(kr)$ is Hankel function,

$$G[\vec{R},u(v),v] = \sqrt{\pi}\mathrm{e}^{\mathrm{i}3\pi/4} f(\vec{R},0,v)w(\mathrm{e}^{\mathrm{i}\pi/4}g)$$

$$+ \frac{1}{g}\left[f(\vec{R},0,v) - \frac{f(\vec{R},u(v),v)}{\mathrm{ch}(u(v)/2)}\right],$$

$$g = \sqrt{2kr}\mathrm{sh}\left(\frac{u(v)}{2}\right),$$

$w(x) = \mathrm{e}^{x^2}\left[1 + (2\mathrm{i}/\sqrt{\pi})\int_0^x \mathrm{e}^{t^2}\,\mathrm{d}t\right]$ is the conventional probability integral of a complex variable (Abramowitz and Stegun, 1964). As a result of stationary phase calculations we arrive at the one-dimensional equation with contour integrals along two lines: the (x,y) plane projection of the propagation line ($u = 0$, $0 < v < \pi$) and the linear boundary $\partial\Omega_p$ ($u = u(v)$) of the local inhomogeneity area. In an operator form this is the following equation:

$$V = V_0 + AV + BV \tag{12}$$

where A is a Volterra operator which acts on the functions $f_t(\vec{R},0,v)$ and $f(\vec{R},0,v)$, and B is a Fredholm operator which acts on the function $f(\vec{R},u(v),v)$. To solve the one-dimensional integral equation (12), we use the numerical–analytical method of semi-inversion (Soloviev and Agapov, 1997). The algorithm of its solution is the formula (13):

$$V^{(0)} = V_0, \quad V^{(m)} = V_0 + AV^{(m)} + BV^{(m-1)}, \tag{13}$$

where $m = 1, 2, 3, \ldots$ is iteration number. We point out that A as a Volterra integral operator, can be easily converted with the aid of the conventional stepwise procedure (e.g., Wagner, 1954). Moreover, it contains the first, dominant term of the asymptotic expansion. Its contribution to the solution in comparison with B is expected to be more significant for a larger value of the parameter kr.

For calculating the field in a uniform waveguide ($\Pi_0(\vec{R})$ and $\Pi_0(\vec{R},\vec{R}')$) the computer program was generated, which computes the absolute value and argument of attenuation function of the vertical component of Hertz's vector for any $0 \leqslant z_t, z \leqslant h$ and $r \geqslant 0$ with a pre-assigned precision. It is full-wave presentation that combines both the ray-expansion method and the normal mode series.

4. Numerical results and discussion

For the numerical simulation of radio wave propagation process on the Tsushima–Inubo path (Hayakawa et al., 1996b) we have chosen the following values of Earth-ionosphere waveguide model: Earth's surface properties are defined by $\sigma = 4.0$ S/m, $\varepsilon_r = 81$ and the path length is about $R \sim 1000$ km. When we have calculated δ_{it} and z_{it} from the given electron density $N_e(z)$ and effective collision frequency $v_e(z)$ height profiles, the geomagnetic field has been allowed for. Certainly, in this case, the electrical properties of anisotropic ionosphere may be described only by a tensor of surface impedance and this tensor cannot be reduced to scalar. If we introduce impedance boundary conditions as:

$\vec{E}_{\tan} = Z_0 \hat{\delta} [\vec{H}_{\tan} \times \vec{n}], \quad \text{where}$

$$Z_0 = \sqrt{\frac{\mu_0}{\varepsilon_0}} \quad \text{and} \quad \hat{\delta} = \begin{pmatrix} \delta^{(e)} & \delta_{12} \\ \delta_{21} & \delta^{(m)} \end{pmatrix},$$

the tensor component which is responsible for TM field scattering into TM, is $\delta_{it} = \delta^{(e)} - \frac{\delta_{12}\delta_{21}}{\delta^{(m)}}$ (Makarov et al., 1994). This last one is that we have used for numerical estimations. The components of geomagnetic field were computed in multipole approximation for the central point on the path. Both the transmitter and receiver (observer location) are assumed to be on the Earth's surface, $z_t = z = 0$. We consider two signal frequencies: $f_1 = 10.2$ kHz and $f_2 = 11.3$ kHz.

The local ionospheric disturbance is simulated by a bell-shaped perturbation of the waveguide ionospheric bound:

$$\Delta h = A_p \exp[-((x - x_p)^2 + (y - y_p)^2)/r_p^2]. \tag{14}$$

The effective radius of perturbation in Eq. (14) is chosen equal to $r_p = 200$ km; the position of disturbance centre with respect to the propagation path corresponds to the great Hyogo-ken Nambu (Kobe) earthquake (January 17, 1995) epicentre and is determined by the following values of the horizontal coordinates $x_p = 464$ km and $y_p = -70$ km (see Fig. 3). We have considered three model disturbances: (1) the depression of upper bound without any impedance perturbation, when $A_p = -3$ km, $\delta_p = \delta_i$; (2) the depression of upper bound with impedance perturbation, when $A_p = -3$ km, $\delta_p = \delta_i + \Delta\delta_p$, $\Delta\delta_p = -0.02$–0.14i; and (3) the elevation of upper bound without any impedance perturbation, when $A_p = +3$ km, $\delta_p = \delta_i$. These concrete values of A_p and $\Delta\delta_p$ were chosen from the intervals $0 \leqslant |A_p| < (z_{it \text{ night}} - z_{it \text{ day}})$ and $0 \leqslant \Delta\delta_p < (\delta_{it \text{ day}} - \delta_{it \text{ night}})$, respectively.

Fig. 4 illustrates the behaviour of amplitude (in the upper panel) and phase (in the lower panel) of attenuation function as a function of local time (LT) since the beginning of sunrise on the path. The signal frequency is 10.2 kHz, and transmitter–receiver distance is 1043 km in the upper panel, while we consider $R = 947$ km in the lower panel. The perturbation of the ionospheric waveguide bound is waveguide wall depression. Hereafter, and in all the following figures, there are two curves in each panel; the solid lines indicate the situations without any local inhomogeneity above the propagation path (only with taking into account the terminator transition), and the dotted lines, the problems with local inhomogeneity (local inhomogeneity against the background of terminator transition). The shift in the amplitude as well as in the phase minimum on the side of lengthening of the day conditions may be seen in both figures. These shifts are found to be around and more than 10 min.

Fig. 5 shows the situation when the local perturbation on the ionospheric waveguide bound is waveguide
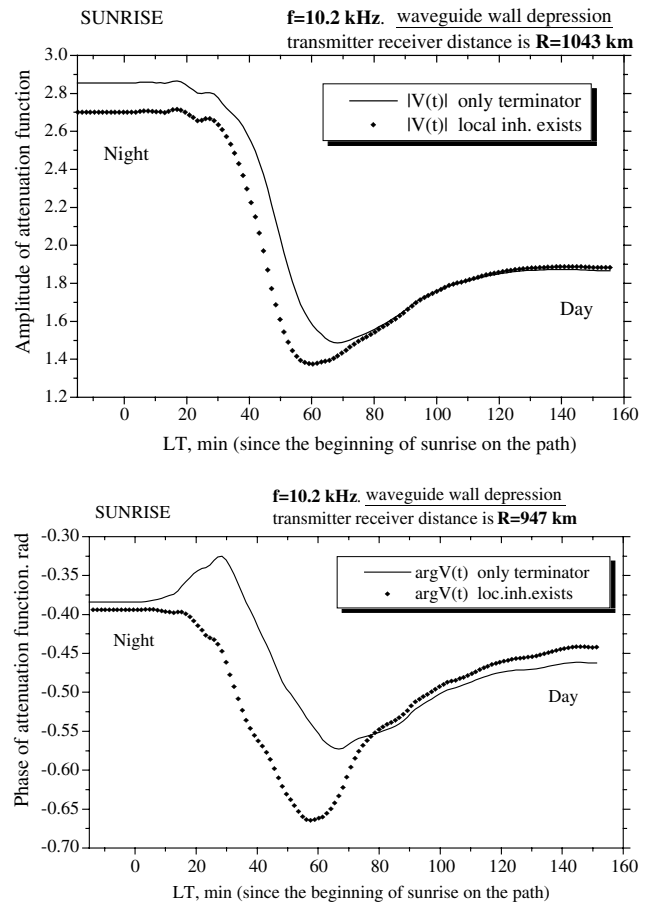

Fig. 4. Amplitude (upper panel) and phase (lower panel) of attenuation function as a function of local time (LT) since the beginning of sunrise on the path. The distance R is 1043 km (upper panel) and 947 km (lower panel). The local perturbation on the ionospheric waveguide bound is waveguide wall depression.

wall elevation. We have found that there are some small signal shifts in the amplitude and phase minimums, but on the side of shortening of the day conditions.

Fig. 6 illustrates the situation when the local perturbation on the ionospheric waveguide bound is waveguide wall depression with impedance perturbation. The signal frequency is 10.2 kHz, and the distance R is 1043 km. In the upper panel for the curves indicate the amplitude of attenuation function and in the lower panel the curves correspond to the phase of attenuation function. The deviation in phase minimum may be evidently defined in the lower panel, which is found to be more than 10 min, and in the same tendency of lengthening of the day conditions.

Next Fig. 7 presents the sunset situation when the signal frequency is 11.3 kHz, the distance R is 1041 km, and the local perturbation on the ionospheric waveguide bound is waveguide wall depression. The upper panel is for the amplitude, while the lower is for the
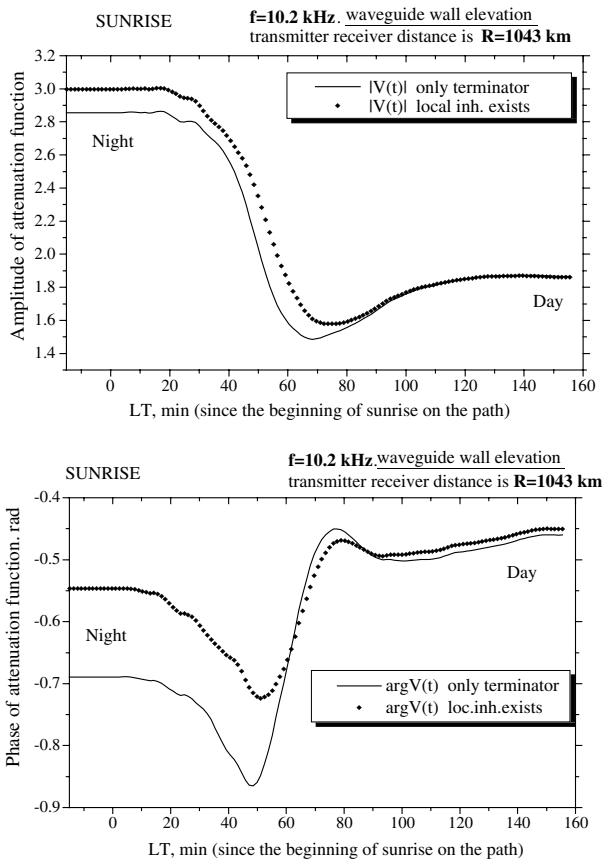
Fig. 5. Amplitude (upper panel) and phase (lower panel) of attenuation function as a function of local time (LT) since the beginning of sunrise on the path. The local perturbation on the ionospheric waveguide bound is waveguide wall elevation.
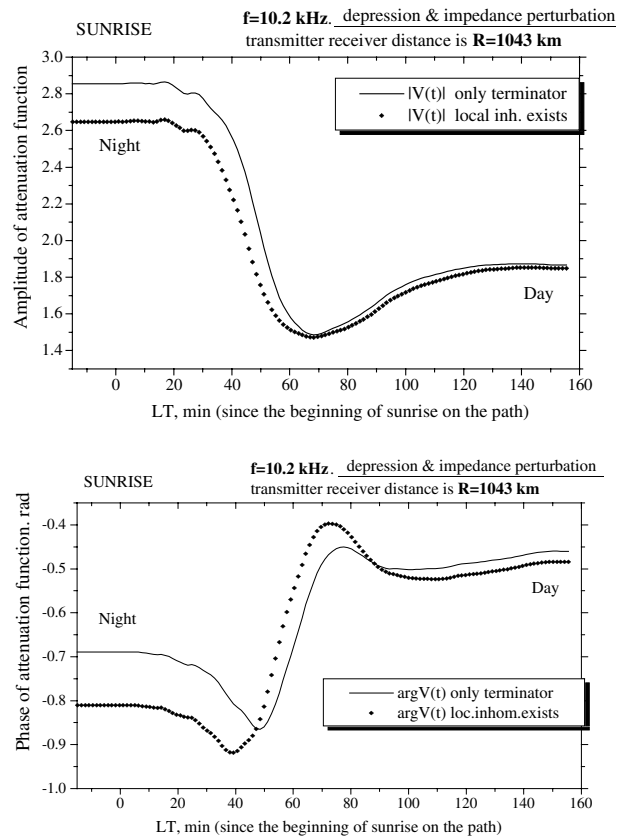

Fig. 6. Amplitude (upper panel) and phase (lower panel) of attenuation function as a function of local time (LT) since the beginning of sunrise on the path. The local perturbation on the ionospheric waveguide bound is waveguide wall depression with impedance perturbation.

phase of the attenuation function. We can see the deviation of minimum only in the phase behaviour but there is no remarkable amplitude minimum. The phase minimum deviation is found to be nearly 10 min, and in the same tendency of lengthening of the day conditions again.

5. Conclusions

It may be concluded that the analysis of the represented results of numerical simulation affirm that the emergence of a local ionosphere inhomogeneity on the radio wave propagation path may be a cause of deformations in the diurnal curves of VLF field amplitude and phase in accordance with the above-mentioned observational data. This local inhomogeneity must be equivalent to the local waveguide wall depression and not the local waveguide wall elevation. In this case only the shift in the amplitude or phase minimum is on the side of lengthening of the day conditions (as in the experiment). This effect is a result

of interaction of multimode field with the complicated waveguide boundary. Therefore, for the observer being placed in a given point and receiving only one frequency, this effect may not be shown (see e.g. Figs. 6 and 7 upper panel). While our attention in this paper is mainly concentrated on the explanation of any seismo-induced VLF effect, we believe that the presented method of 3-D VLF field diffraction itself could be useful for a wider scope of the effects related to VLF propagation in the inhomogeneous ionosphere, e.g. Trimpi effect (Baba et al., 1998; Soloviev and Hayakawa, 2002).
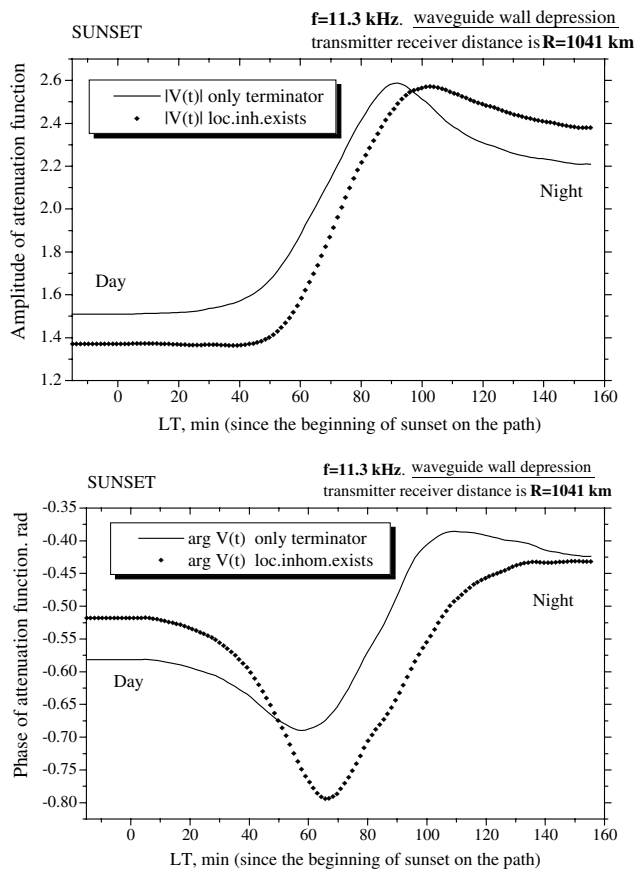
Acknowledgements

Fig. 7. Amplitude (upper panel) and phase (lower panel) of attenuation function as a function of local time (LT) since the beginning of sunset on the path. Signal frequency is 11.3 kHz, the distance R is 1041 km, and the local perturbation on the ionospheric waveguide bound is waveguide wall depression.

References

Abramowitz, M., Stegun, I., 1964. Handbook of Mathematical Functions. U.S. Government Printing Office, Washington, DC.

Baba, K., Nunn, D., Hayakawa, M., 1998. The modeling of VLF Trimpis using both finite element and 3D Born modeling. Geophys. Res. Lett. 25, 4453–4456.

Clilverd, M.A., Rodger, C.J., Thomson, N.R., 1999. Investigating seismoionospheric effects on a long subionospheric path. J. Geophys. Res. 104 (A12), 28171–28179.

Earth's Lower Ionosphere, 1995. The model of the global distribution of electron density and effective collision frequency for low-frequency radio wave propagation (electromagnetic field) prediction, GOST R 25645.157-94. Standards Press, Moscow, 380 pp.

Ferguson, J.A., Snyder, F.P., 1990. Computer programs for assessment of long wavelength radio communications. Tech. Doc. 1773, National Ocean System Center, Alexandria, Va.

Fihtenholtz, G.M., 1969. In: Course in the Differential and Integral Calculus, vol. III. Nauka, Moscow.

Fok, V.A., 1965. Electromagnetic Diffraction and Propagation Problems. Pergamon, NY.

Galejs, J., 1971. VLF propagation across discontinuous day-time to night-time transitions in anisotropic terrestrial waveguide. IEEE Trans. Ant. Prop. 19, 756–762.

Galuk, Yu.P., Ivanov, V.I., 1978. The characteristics of VLF propagation in the Earth-ionosphere waveguide. In: Problemy Difrak-
tsii i Rasprostraneniya Voln, 16. St. Petersburg Univ. Press, St. Petersburg, pp. 148–152.

Hayakawa, M., 2001. NASDA's Earthquake remote sensing frontier research; Seismo-electromagnetic phenomena in the lithosphere, atmosphere and ionosphere, Final report, March 2001, p. 228.

Hayakawa, M., Molchanov, O.A. (Eds.), 2002. Seismo Electromagnetics, Lithosphere–Atmosphere–Ionosphere Coupling. Terrapub, Tokyo. p. 477.

Hayakawa, M., Molchanov, O.A., Ondoh, T., Kawai, E., 1996a. The precursory signature effect of the Kobe earthquake on VLF subionospheric signals. J. Comm. Res. Lab. 43, 169–180.

Hayakawa, M., Molchanov, O.A., Ondoh, T., Kawai, E., 1996b. Precursory signature of the Kobe earthquake on VLF subionospheric signal. J. Atmos. Electr. 16 (3), 247–257.

Makarov, G.I., Novikov, V.V., Rybachek, S.T., 1994. Radio Wave Propagation in the Earth-Ionosphere Waveguide and in the Ionosphere. Nauka, Moskow. 152pp.

Molchanov, O.A., Hayakawa, M., 1998. Subionospheric VLF signal perturbations possibly related to earthquakes. J. Geophys. Res. 103 (A8), 17489–17504.

Molchanov, O.A., Hayakawa, M., Ondoh, T., Kawai, E., 1998. Precursory effects in the subionospheric VLF signals for the Kobe earthquake. Phys. Earth Planet. Int. 105, 239–248.

Molchanov, O.A., Hayakawa, M., Miyaki, K., 2001. VLF/LF sounding of the lower ionosphere to study the role of atmospheric oscillations in the lithosphere–ionosphere coupling. Adv. Polar Upper Atmos. Res. 15, 146–158.

Nikolaenko, A.P., Hayakawa, M., Molchanov, O.A., 1999. Geometrical model for the VLF precursory signal at the propagation path Tsushima–Inubo before the Kobe earthquake. In: Hayakawa, M. (Ed.), Atmospheric and Ionospheric Electromagnetic Phenomena Associated with Earthquakes. Terrapub, Tokyo, Japan, pp. 451–458.

Novikov, V.V., Rybachek, S.T., 1997. The effect of a transverse irregularity on the electromagnetic fields excited by VLF transmitters at ionospheric heights in the Earth-ionosphere waveguide near the terminator. J. Atmos. Solar-Terr. Phys. 59 (12), 1453–1459.

Orlov, A.B., Pronin, A.E., Uvarov, A.N., 2000. The electron density of lower ionosphere profile modelling according to the VLF propagation data. In: Problemy Difraktsii i Rasprostraneniya Voln, 28. St. Petersburg Univ. Press, St. Petersburg, pp. 83–114.

Pappert, R.A., Morfitt, D.G., 1975. Theoretical and experimental sunrise mode conversion results at VLF. Radio Sci. 10, 537–546.

Rodger, C.J., Clilverd, M.A., 1999. Modeling of subionospheric VLF signal perturbations associated with earthquakes. Radio Sci. 34, 1177–1185.

Smith, R., 1977. Mode conversion coefficients in the Earth-ionosphere waveguide for VLF propagation below a horizontally stratified anisotropic ionosphere. J. Atmos. Terr. Phys. 39, 539–543.

Somsikov, V.M., Ganguly, B., 1995. On the formation of atmospheric inhomogeneities in the solar terminator region. J. Atmos. Solar-Ter. Phys. 57 (12), 1513–1523.

Soloviev, O.V., 1998. Low frequency radio wave propagation in the Earth-ionosphere waveguide perturbed by a large-scale three-dimensional inhomogeneity. Izv. Vyssh. Uchebn. Zaved. Radiofiz. 41 (5), 588–604.

Soloviev, O.V., 1999. Depolarization of the electromagnetic field scattered by a three-dimensional large-scale irregularity of the lower ionosphere. Izv. Vyssh. Uchebn. Zaved. Radiofiz. 42 (5), 418–430.

Soloviev, O.V., 2000. Depolarization of the electromagnetic field in a locally inhomogeneous Earth-ionosphere waveguide. Izv. Vyssh. Uchebn. Zaved. Radiofiz. 43 (7), 617–629.

Soloviev, O.V., Agapov, V.V., 1997. An asymptotic three-dimensional technique to study radio wave propagation in the presence of a localized perturbation of environment. Radio Sci. 32 (2), 515–524.

Soloviev, O.V., Hayakawa, M., 2002. Three-dimensional subiono-spheric VLF field diffraction by a truncated high conducting cylinder and its application to Trimpi effect problem. Radio Sci. 37 (5), 4, doi:10.1029/2001RS002499.

Wagner, C., 1954. On the numerical solution of Volterra integral equations. J. Math. Phys. 32 (4), 289–301.

Wait, J.R., 1968a. Mode conversion and reflection effects in the Earth-ionosphere waveguide for VLF radio waves. J. Geophys. Res. 73, 3537–3548.

Wait, J.R., 1968b. Note on mode conversion at VLF in the Earth-ionosphere waveguide. J. Geophys. Res. 73, 5801–5804.